ELSEVIER

Catalysis Today 64 (2001) 51–58

CATALYSIS TODAY

www.elsevier.com/locate/cattod

Silicon nitride supported platinum catalysts for the partial oxidation of methane at high temperatures

F. Monnet, Y. Schuurman*, F. Cadete Santos Aires, J.C. Bertolini, C. Mirodatos

Institut de Recherches sur la Catalyse (UPR-CNRS), 2 Avenue Albert Einstein, F-69626 Villeurbanne Cedex, France

Abstract

The catalytic partial oxidation of methane has been studied over platinum silicon nitride supported catalysts in the temperature range of 900–1100°C at a contact time of 0.35 ms at atmospheric pressures. The feed consisted of a mixture of $CH_4/O_2/N_2 \approx 2/1/10$. The catalysts were prepared by impregnation of platinum bis-acetyl-acetonate on silicon nitride powder (Si_3N_4). The different catalysts were characterized by chemical analysis, XPS and TEM. Minor particle sintering occurs during reaction. Metal losses were observed at 900°C, for catalysts containing 1.0 and 2.2 wt.% of platinum. A catalyst with a low amount of platinum (0.045 wt.%) appeared to be stable at 900°C, as no platinum loss was observed. The high stability of the 0.045 wt.% Pt/Si_3N_4 catalyst could be attributed to particular interactions between the metal and the support.

Keywords: Partial oxidation; Methane; Synthesis gas; Silicon nitride; Platinum; Deactivation

1. Introduction

Methane conversion is an important area of research because of the need for an efficient utilization of natural gas reserves. Recently [1–7], a lot of research has been devoted to short contact time reactors for the direct partial oxidation of methane. Their main advantages are reduced volume and autothermal operation.

The reported operating conditions [5–9] that favor the direct partial oxidation are high temperatures (≈1000°C) and very short contact times ($\approx 10^{-4}$ s). Catalysts that are employed for this kind of operations include bulk platinum or rhodium as well as platinum or rhodium supported on refractory ceramic materials. Under such severe conditions, platinum in particular but also rhodium catalysts exhibit important metal losses. Different problems of deactivation occur by restructuration of bulk materials and volatilization and/or sintering on supported Pt and Rh [5–7,10,11].

The objective of this study is to develop a platinum catalyst showing improved stability at high temperatures. For this purpose, platinum supported on low specific surface area ceramic materials, which are stable at high temperatures, was employed. Silicon nitride has a high melting point and is chemically inert. Its exceptional thermal conductivity, especially at high temperatures, between two and three times better than alumina, should help to avoid hot spot formation [12,13]. The current study focuses on the morphology and the behavior of these Pt/Si_3N_4 catalysts.

2. Catalysts preparation

All catalysts were prepared by impregnation of a low specific surface area (8.8 $m^2\,g^{-1}$) silicon nitride

---

* Corresponding author. Tel.: +33-472-445-482;
fax: +33-472-445-399.
E-mail address: schuurma@catalyse.univ-lyonl.fr (Y. Schuurman).

0920-5861/01/$ – see front matter © 2001 Elsevier Science B.V. All rights reserved.
PII: S0920-5861(00)00508-3

support (Goodfellow) with a solution of platinum bis-acetyl-acetonate (Strem Chemicals).

The platinum bis-acetyl-acetonate complex was dissolved in toluene (100 ml) at room temperature. The silicon nitride powder was added to the solution and stirred for 24 h. The solvent was evaporated and the residue was dried under vacuum at 80°C. The catalyst was first heated in an argon flow at 500°C for 2 h and cooled down. Then the sample was heated in an oxygen flow at 350°C again for 2 h and cooled down to eliminate the rest of the ligands. Finally, a hydrogen flow at 500°C for 2 h was passed over the sample to reduce the metal.

By this method, three platinum based catalysts were prepared with increasing amounts of metal. They contained, respectively, 0.045, 1.0 and 2.2 wt.% of Pt as measured by chemical analysis. This preparation method led to dispersions varying between 16 and 100%, depending on the platinum metal content (see Table 1). The silicon nitride particles are agglomerates of much smaller particles and the 0.2–0.3 mm sieve fractions were used.

All these catalysts were extensively characterized by chemical analysis (ICP measurement), X-ray photoelectron spectroscopy (XPS) and transmission electron microscopy (TEM) before and after reaction at 900°C.

3. Experiments

The experiments were performed in a tubular quartz reactor with an internal diameter of 11 mm. A K-type thermocouple located in the catalytic zone was used for temperature measurement and control. One hundred milligram catalyst samples were used for each experiment and packed between two layers of quartz wool. The reactants, methane (99.99%), oxygen (99.9%) and nitrogen (99.99%) (Air Liquide), were used without further purification. For all the experiments a 2/1/10 ratio of a mixture of $CH_4/O_2/N_2$ was maintained. Flows were controlled by mass flowcontrollers (Brooks) and maintained at 1600 ml min^{-1}. This corresponds to a GHSV of 5×10^5 h^{-1}. The catalytic zone was heated by a short furnace ($h = 50$, $\phi = 50$ mm) in order to avoid gas phase reactions. The length of the catalytic zone, less than 2 mm should favor isothermal operation.

The catalysts were pre-treated initially in an oxygen flow for 1 h at 500°C and then in a hydrogen flow for 1 h at 500°C. The temperature was then increased to 900°C under an inert nitrogen flow.

Analysis of the gas mixture was carried out by periodically directing the reactor effluent through a sample loop of an HP 5890 gas chromatograph equipped with two thermal conductivity detectors (TCDs) and configured with four columns in a series/parallel arrangement. Water was removed from the other components at the end of the reactor by means of a condenser. In the first line, carbon dioxide was separated on a Porapak Q column while methane, carbon monoxide, oxygen, nitrogen were separated on a molecular sieve using helium as a carrier gas. Nitrogen was used as an internal standard.

In the second line with nitrogen as carrier gas, hydrogen and methane were analyzed. The analysis of methane on both systems was used to correct for the two different injection volumes.

4. Characterization

Chemical analysis was carried out with an inducted coupled plasma (ICP) spectrometer. The platinum from the samples was dissolved successively in a mixture, $H_2SO_4/HNO_3/HF$ and $HF/HCl/HNO_3$. These acidic treatments did not dissolve the silicon nitride support and a white-gray residue was observed. The solutions of platinum were analyzed with a Spectroflamme D (Spectro). The ICP results of the platinum content, summarized in Tables 1 and 2, are within 2% of the theoretical platinum loading.

XPS studies were performed using an ESCALAB 200R machine (Fisons Instruments) using the Mg Kα line (1253.6 eV) as excitation source. The N 1s peak at 397.6 eV of the silicon nitride support was used as an internal standard.

TEM experiments were performed with a JEOL 2010 microscope working at 200 keV and equipped with an UHR pole-piece. The supported catalysts were dispersed in ethanol in an ultrasonic bath. A drop of this suspension was disposed on a holey-carbon thin film supported on a microscopy copper grid (3.05 mm, 200 mesh). The platinum particle size distributions were determined from the micrographs. A large number of particles, 250 for the 0.045 wt.% platinum

Table 1
Main features of the Pt/Si_3N_4 catalysts before reaction

Samples	Expected Pt content (wt.%)	Real Pt content (wt.%)	Average particle size (nm)	% Pt 4f / % Si 2p[a]	Pt $4f_{7/2}$ binding energy (eV)
0.045 wt.% Pt	0.5	$0.045 \pm 9 \times 10^{-4}$	1.1	0.002	72.4
1.0 wt.% Pt	1.4	$1.0 \pm 2 \times 10^{-2}$	5.0	0.043	71.6
2.2 wt.% Pt	2.5	$2.2 \pm 4 \times 10^{-2}$	6.4	0.083	71.4

[a] Peak areas corrected for the platinum and silicon sensitivity factors.

Table 2
Main features of the Pt/Si_3N_4 catalysts after 4 h on stream at 900°C

Samples	Pt content after reaction (wt.%)	Average particle size (nm)	% Pt 4f / % Si 2p[a]	Pt $4f_{7/2}$ binding energy (eV)
0.045 wt.% Pt	$0.046 \pm 9 \times 10^{-4}$	2.8	–	–
1.0 wt.% Pt	$0.5 \pm 1 \times 10^{-2}$	5.4	0.020	71.2
2.2 wt.% Pt	$0.88 \pm 2 \times 10^{-2}$	6.5	0.039	71.2

[a] Peak areas corrected for the platinum and silicon sensitivity factors.

catalyst and 600 for the 1.0 and 2.2 wt.% platinum catalysts, were counted and their sizes were measured. The average particle size was calculated according to the following equation:

$$\overline{d_{Pt}} = \frac{\sum n_i d_i}{\sum n_i} \qquad (1)$$

where $\overline{d_{Pt}}$ is the average particle size (m), n_i the number of particles corresponding to a diameter of d_i (m).

5. Results

5.1. Catalyst characterization before reaction

Chemical analysis revealed that the real amount of platinum loaded is approximately 0.4 wt.% lower than the amount of platinum originally introduced in the preparation solution.

A micrograph of the 0.045 wt.% platinum catalyst, shown in Fig. 1, clearly shows the presence of small spherical particles with a size of approximately 1 nm randomly dispersed on the surface. No region free of particles and no coating of the platinum by the support were evidenced. Fig. 2 shows that the particle size distribution for the 0.045 wt.% sample is rather narrow. The average particle sizes as determined by Eq. (1) are summarized in Table 1. The average particle size increases with increasing platinum content.

Fig. 3 shows the XPS region of the platinum 4f doublet. The binding energy of the Pt $4f_{7/2}$ changes slightly with increasing platinum content (Table 1). For all catalysts the binding energy observed was slightly higher than that of bulk platinum (71.1 eV) [14]. The higher binding energy (72.4 eV) was observed for the lowest content catalyst. The Pt 4f/Si 2p ratio values are consistent with the platinum content determined by chemical analysis.

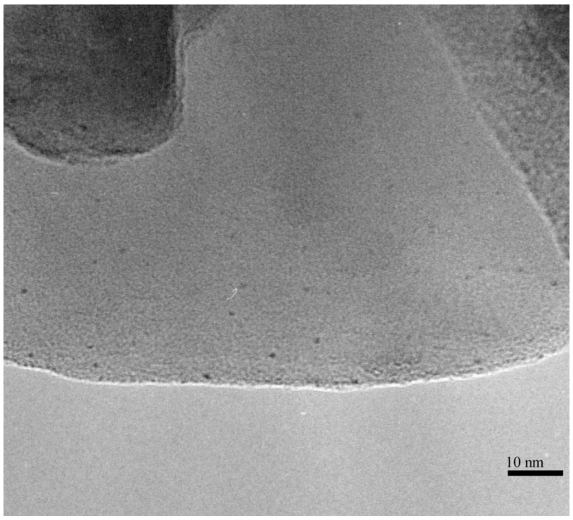

Fig. 1. Micrograph of the 0.045 wt.% Pt/Si_3N_4 catalyst before reaction.

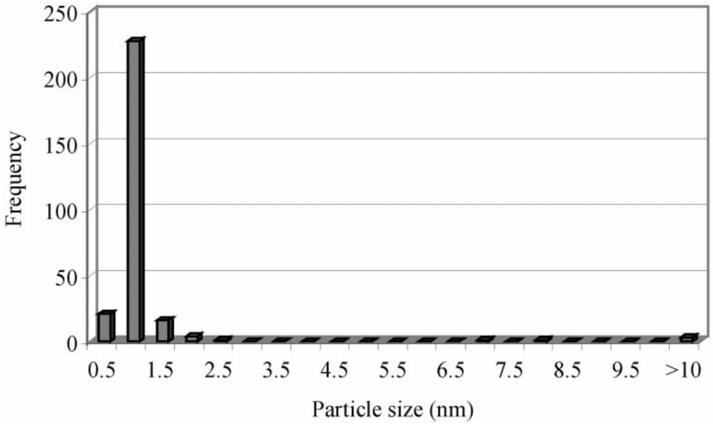

Fig. 2. Particle size distribution of the 0.045 wt.% Pt/Si_3N_4 catalyst before reaction.

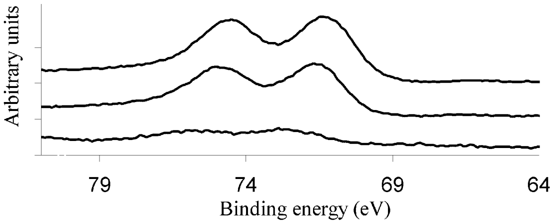

Fig. 3. XPS spectra of the Pt 4f doublet region before reaction: (a) 0.045 wt.% Pt/Si_3N_4; (b) 1.0 wt.% Pt/Si_3N_4; (c) 2.2 wt.% Pt/Si_3N_4 catalysts.

5.2. *Catalyst characterization after reaction*

After 4 h on stream at 900°C the catalysts were characterized ex situ by chemical analysis, TEM and XPS. Chemical analysis of the platinum content after reaction revealed that a significant platinum loss had occurred for the 1.0 and 2.2 wt.% samples (Table 2). In contrast the 0.045 wt.% catalyst did not present any platinum loss during the reaction.

A micrograph of the 0.045 wt.% platinum catalyst after reaction (Fig. 4) shows an increased average particle size (see also Table 2). Almost no particles larger than 5.0 nm were observed. The particles are still evenly distributed over the silicon nitride support and do not seem to be coated by the support.

Fig. 5 shows the particle size distribution after reaction for the 0.045 wt.% platinum catalyst. The average particle size has increased and the width of the particle size distribution has become broader. This trend in the shape of the particle size distribution was observed for all three catalysts.

The XPS spectra in the Si 2p region are identical for all catalysts after reaction at 900°C. It can be decomposed into two peaks centered at 101.8 and 103.2 eV characteristic, respectively, of the silicon in Si_3N_4 and SiO_2 compounds. The signal corresponding to the Si_3N_4 represents about 77% of the total Si signal.

Pt $4f_{7/2}$ binding energies as observed by XPS, shown in Fig. 6 for the 1.0 and 2.2 wt.% catalysts

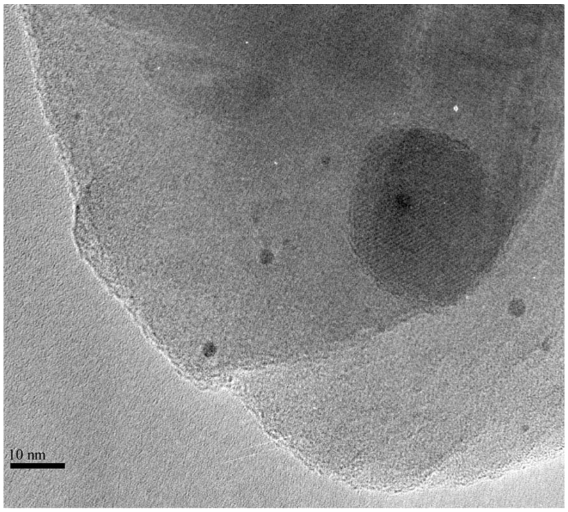

Fig. 4. Micrograph of the 0.045 wt.% Pt/Si_3N_4 catalyst after 4 h of time on stream at 900°C.

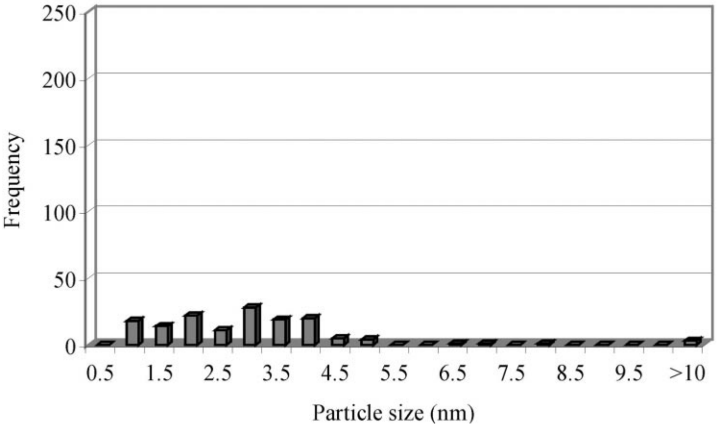

Fig. 5. Particle size distribution after 4 h of time on stream at 900°C for the 0.045 wt.% Pt/Si_3N_4 catalyst.

have decreased after reaction to a value of 71.2 eV, similar to the value of bulk platinum [14]. A quantitative analysis showed that the Pt 4f signal intensity for these two samples was approximately two times lower than before reaction (Table 2). The XPS spectrum of the 0.045 wt.% sample did not allow an accurate measurement of the binding energies due to the low signal to noise ratio (Fig. 6).

5.3. Catalyst performance

Blank experiments, between 900 and 1100°C were performed using only the silicon nitride support inserted between quartz wool at a 1600 ml min^{-1} total flow of $CH_4/O_2/N_2$ (2/1/10) mixture. Both methane and oxygen conversions at 900°C were less than 1% and remained less than 6% at 1100°C.

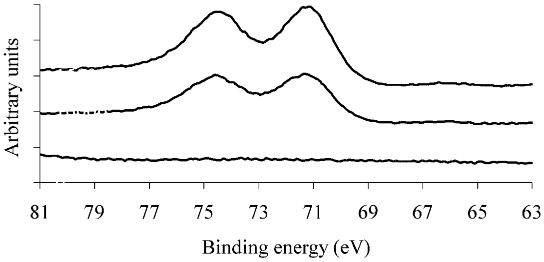

Fig. 6. XPS spectra in the Pt 4f doublet region after 4 h of time on stream at 900°C: (a) 0.045 wt.% Pt/Si_3N_4 catalysts; (b) 1.0 wt.% Pt/Si_3N_4 catalysts; (c) 2.2 wt.% Pt/Si_3N_4 catalysts.

In Fig. 7a and b methane and oxygen conversions are shown as a function of time on stream for a 4 h experiment. Both the conversions of methane and oxygen decrease with time on stream for the 1.0 and 2.2 wt.% samples while they initially increase and then remain constant for the 0.045 wt.% sample.

Fig. 7c and d shows the selectivity to carbon monoxide and hydrogen versus time on stream. The carbon monoxide selectivity is constant with time on stream for the 1.0 wt.% catalyst. It slightly increases during the first 100 min of the experiment and then remained constant for the 0.045 and 2.2 wt.% samples. The hydrogen selectivity decreases for the 1.0 wt.% while it is constant for the two other catalysts.

6. Discussion

Stability of the silicon nitride support appears to be excellent under a flow of $CH_4/O_2/N_2$ at high temperatures, 900–1100°C. Blank experiments performed with the silicon nitride support showed that it is totally inactive in the temperature range of 900–1100°C. XPS analysis of the Si 2p region performed after this experiment confirms the good chemical inertia of the silicon nitride support. Only a thin surface oxidation film (1–2 nm) was determined by XPS and confirmed by TEM micrographs. Using high gas flows and a short hot zone, about 3 cm, methane and oxygen conversions in the gas phase could be kept below 6%.

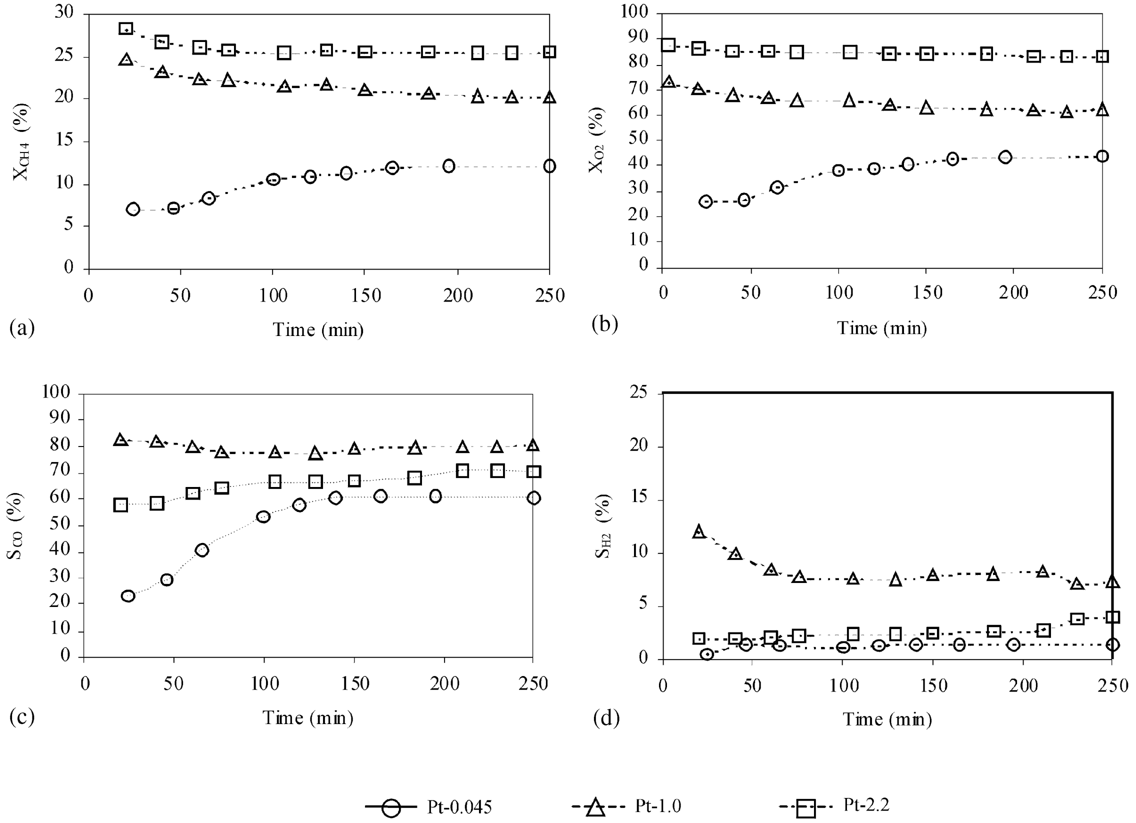

Fig. 7. Effect of time on stream at 900°C and a $CH_4/O_2/N_2$ feed ratio of 2/1/10 on: (a) methane conversion; (b) oxygen conversion; (c) carbon monoxide selectivity; (d) hydrogen selectivity.

From Tables 1 and 2, summarizing the main features of the catalysts before and after reaction, two phenomena are observed:

1. The average particle size increases, i.e. particle sintering.
2. The XPS and chemical analysis show a loss in the platinum content.

Moreover, these phenomena appear to be a function of the initial platinum content. Whereas the 2.2 wt.% catalyst loses 60% of its initial platinum, the 0.045 wt.% catalyst does not lose any platinum. At the same time, for the 1.0 and 2.2 wt.% catalysts no significant particle sintering was observed by TEM analysis whereas for the 0.045 wt.% the average particle size is three times larger than that before reaction (Tables 1 and 2). Quantitative XPS analysis confirmed such observations. Both sintering processes and metal loss are well known for precious metal catalysts under oxidative conditions [5,7,10,11,15–18]. Metal loss is thought to occur for platinum catalysts at high temperatures due to the volatilization of PtO_2 (16–18). For the current samples, the two following processes appear to take place simultaneously: the smallest particles are undergoing sintering to yield larger particles and the large particles are shrinking due to platinum loss by volatile PtO_2. For the 1.0 and 2.2 wt.% samples the result is an apparent stable particle size. The stability of the 0.045 wt.% sample may be related to a particle size effect. An argument for this explanation is the significantly different binding energy for the 0.045 wt.% sample compared to the other two catalysts. The shift of 0.8–1.0 eV of the Pt $4f_{7/2}$ binding energy might be related to some small particle size effect and/or to a peculiar platinum support interaction which could lead to the formation of a compound of Pt_2Si-type [14]. This might prevent the small platinum oxide particles, 1–3 nm, from becoming volatile.

Support interactions are also reported in a recent study by Hwang and Yeh [10]. They carried out a study on alumina and silica supported platinum catalysts. They reported that PtO_2 sublimation for platinum supported on silica is more significant than for platinum supported on alumina. They explained it by considering structural modifications between platinum oxide (PtO and PtO_2) and alumina which can lead to a more stable spinel structure $PtAl_2O_4$. They claimed that highly dispersed platinum particles on SiO_2 are more easily converted into PtO_2 than those on Al_2O_3.

The evolution of the methane conversion with time on stream is well in line with the results of the catalyst characterization. The two samples of higher loading samples show a decrease in the methane conversion. This deactivation could not be attributed to a carbon deposition onto the surface but is instead, as evidenced by the catalyst characterization, due to the decrease of the platinum surface area. Mass balances are close to 100% and the micrographs (Fig. 4) after reaction do not reveal the presence of any graphitic carbon covering the platinum particle or any amorphous carbon whiskers. In addition, XPS spectra in the C 1s region remain symmetric. The XPS area of C 1s signal remains constant (3% of the atomic composition) before and after reaction. It corresponds to a carbon pollution usually observed when XPS characterization is performed ex situ.

For the 0.045 wt.% sample the methane conversion actually increases with time on stream. This increase in activity is accompanied by a similar increase in the selectivity to both hydrogen and carbon monoxide. The oxygen–platinum bond strength increases with decreasing particle size [19–22]. Therefore the oxygen surface coverage of the small platinum particles will be higher than that of the larger ones. A high oxygen surface coverage has two effects on the methane oxidation: it lowers the available number of methane adsorption sites and it favors consecutive oxidation of carbon monoxide and hydrogen. Whatever the particle size, at incomplete oxygen conversion, the selectivity to hydrogen remains low. A high concentration of adsorbed oxygen species allows fast secondary oxidation reactions of adsorbed hydrogen [23].

Thus the sintering of the 0.045 wt.% sample enhances its catalytic performance by increasing both its activity and selectivity. This trend levels off for the larger particles since the selectivity obtained with the 1.0 and 2.2 wt.% samples is close to the 0.045 wt.% sample after sintering.

As discussed before, deactivation due to particle sintering is usually observed in an oxidative atmosphere and at high temperatures. Recently, Yamamoto and Uchida [24] showed that Pt, Pd and Pt–Pd monolith catalysts supported on alumina when exposed to an oxidative mixture of $CH_4/O_2/H_2O$ (0.3, 4.9 and 14%) at a temperature of 673 K exhibited rapid deactivation. The highest loaded samples showed the most pronounced deactivation. According to the authors the deactivation could not be attributed to the formation of coke (large excess of oxygen), but rather to particle sintering. However, they did not give any details about possible platinum loss during the experiment. The 1.0 wt.% Pt/Si_3N_4 catalyst presented here shows a much better behavior. As a matter of fact, its deactivation remains less than 20% after 50 h under a $CH_4/O_2/N_2$ (2/1/10) flow at a temperature of 1173 K.

7. Conclusions

The employed preparation method using platinum bis-acetyl-acetonate leads to highly dispersed catalysts, at low platinum loading the dispersion can reach up to 100%. Above 900°C on silicon nitride supported catalysts, two processes take place that lead to a decrease of the available surface area:

1. sintering of the small platinum particles,
2. oxidation of the larger particles and subsequent volatilization of PtO_2.

The latter process was not observed for the catalyst containing particles in the range of 1.1 nm. However, these particles sinter to an average size of 2.8 nm after 4 h of time on stream. At the same time, the catalyst activity and selectivity increase when the average particle size increases from 1 to 3 nm and level off at larger particle sizes.

Acknowledgements

This work was supported by CNRS program “Catalyse et Catalyseurs pour l’Industrie et l’Environnement”.

The help of Marie-Thérèse Gimenez for the preparation of the catalysts and that of Michèle Brun for the XPS experiments is greatly acknowledged.

References

[1] P.D.F. Vernon, M.L.H. Green, A.K. Cheetham, A.T. Ashcroft, Catal. Lett. 6 (1990) 181.

[2] Y.F. Chang, H. Heinemann, Catal. Lett. 21 (1993) 215.

[3] F. van Looij, E.R. Stobbe, J.W. Geus, Catal. Lett. 50 (1998) 59.

[4] M. Prettre, C. Eichner, M. Perrin, Trans. Faraday Soc. 42 (1946) 335.

[5] D.A. Hickman, L.D. Schmidt, AIChE J. 39 (1993) 1164.

[6] E.P.J. Mallens, J.H.B.J. Hoebink, G.B. Marin, Catal. Lett. 33 (1995) 291.

[7] K. Heitness, S. Lindberg, O.A. Rokstad, A. Holmen, Catal. Lett. 36 (1996) 25.

[8] O.V. Buyevskaya, K. Walter, D. Wolf, M. Baerns, Catal. Lett. 38 (1996) 81.

[9] C.T. Au, H.Y. Wang, J. Catal. 167 (1997) 337.

[10] C.-P. Hwang, C.-T. Yeh, J. Catal. 182 (1999) 48.

[11] R.M.J. Friedorow, B.S. Chahar, S.E. Wanke, J. Catal. 51 (1978) 193.

[12] D. Dissanayake, M. Rosynek, J.H. Lunsford, J. Phys. Chem. 97 (1993) 3644.

[13] C. Méthivier, J. Massardier, J.C. Bertolini, Appl. Catal. A 182 (1999) 337.

[14] J.F. Moulder, W.F. Strickle, P.E. Sobol, K.D. Bomben, Handbook of X-ray Photoelectron Spectroscopy, Jill Chastain, USA, 1992, p. 181.

[15] P.C. Flynn, S.E. Wanke, J. Catal. 34 (1974) 400.

[16] E.J. Nowak, Chem. Eng. Sci. 24 (1969) 421.

[17] R.W. McCabe, T. Pignet, L.D. Schmidt, J. Catal. 32 (1974) 114.

[18] A.R. McCabe, G.D.W. Smith, A.S. Pratt, Plat. Met. Sci. 30 (1986) 54.

[19] R.W. McCabe, C. Wong, H.S. Woo, J. Catal. 114 (1988) 354.

[20] N.I. Jeager, A.L. Jourdan, G. Schulz-Ekloff, A. Svensson, Stud. Surf. Sci. Catal. 48 (1988) 503.

[21] M.L. Sattler, P.N. Ross, Ultramicroscopy 20 (1986) 21.

[22] F. Parmigiani, E. Kay, P.S. Bagus, Electron Spectrosc. Relat. Phenom. 50 (1990) 39.

[23] M. Fathi, F. Monnet, Y. Schuurman, A. Holmen, C. Mirodatos, J. Catal. 190 (2000) 439.

[24] H. Yamamoto, H. Uchida, Catal. Today 45 (1998) 147.